Plant Physiology and Biochemistry 139 (2019) 528–539

Contents lists available at ScienceDirect

Plant Physiology and Biochemistry

journal homepage: www.elsevier.com/locate/plaphy

Research article

Transcriptome analyses reveal key genes involved in skin color changes of 'Xinlimei' radish taproot

Tongjin Liu[a], Youjun Zhang[a], Xiaohui Zhang[a], Yuyan Sun[b], Haiping Wang[a], Jiangping Song[a], Xixiang Li[a,*]

[a] Institute of Vegetables and Flowers, Chinese Academy of Agricultural Sciences; Key Laboratory of Biology and Genetic Improvement of Horticultural Crops, Ministry of Agriculture, Beijing, PR China
[b] Institute of Vegetables, Zhejiang Academy of Agricultural Sciences, Hangzhou, 310021, PR China

ARTICLE INFO

Keywords:
Radish
Skin color changes
Transcriptome
Anthocyanin
Chlorophyll

ABSTRACT

The color of radish (*Raphanus sativus*) taproot skin is an important visual quality. 'Xinlimei' radish is a red-fleshed cultivar with skin that changes color from red to white and finally to green at the mature stage, and appearance quality is strongly affected if the red color does not fade completely on a single taproot or simultaneously among different taproots. In the present study, anthocyanin and chlorophyll contents and the transcriptome of radish taproot skin at three distinct coloration stages were analyzed to explore the mechanism of color changes. The results showed that decreased anthocyanin and increased chlorophyll contents correlated with the color-fading process. Kyoto Encyclopedia of Genes and Genomes enrichment analysis of differentially expressed genes indicated that anthocyanin and chlorophyll metabolism pathways play important roles in color changes. In red color-fading process, the expression levels of anthocyanin biosynthetic genes (except *PAL* and *C4H*), a transport gene (*RsTT19*), and two anthocyanin biosynthesis transcription factors (TFs), *RsMYB1* and *RsTT8*, were significantly downregulated, whereas peroxidase-encoding genes were significantly upregulated. In the skin-greening process, expression of most chlorophyll biosynthetic genes and two TFs (*RsGLK1* and *RsGLK2*) that likely positively regulate chlorophyll biosynthesis was significantly upregulated. Thus, changes in the expression of these genes may be responsible for the color changes that occur in 'Xinlimei' taproot skin. This is the first report on the roles of chlorophyll metabolism genes and their dynamic relationship with anthocyanin metabolism genes in radish. The findings provide valuable information and theoretical guidelines for improving the appearance quality of 'Xinlimei' radish taproots.

1. Introduction

Radish, belonging to the family Brassicaceae (Cruciales), genus *Raphanus*, is extensively cultivated in Asian countries, and the plants are grown for their taproots, seed oil and sprouts. The skin color of radish taproots is an important visual quality character that directly affects consumer choice behavior. An abundance of varieties with different taproot skin colors, e.g., white, green, red, purple, pink and even black and yellow, are available. Among them, 'Xinlimei' is a China-specific cultivar with green skin and red flesh after maturation that is becoming increasingly popular with consumers due to abundant levels of glucosinolate and anthocyanin, which have health benefits in humans (Park et al., 2011; Sun et al., 2018). The skin color of the 'Xinlimei' taproot is red during the early developmental period and gradually changes to green during maturation. However, in some cases, the red color does not fade completely in a taproot or simultaneously among different taproots, resulting in a dappled or ununiform color at the mature stage (Fig. S1), which can significantly affect its appearance quality. Moreover, the molecular mechanisms leading to red color fading and greening in the 'Xinlimei' radish taproot skin are largely unknown, hindering genetic improvement of its appearance quality and application of high-quality cultivation methods.

Color change is determined by both the biosynthesis and degradation of pigments, and the key pigments affecting red and green color in plants are anthocyanin and chlorophyll, respectively (Lai et al., 2015). Previous research has shown that color fading in 'Red Bartlett' pear is caused by a decrease in the anthocyanin content (Wang et al., 2017a,b), and degreening and pigmentation in *Litchi chinensis* is caused by rapid

* Corresponding author. Institute of Vegetables and Flowers, Chinese Academy of Agricultural Sciences, Beijing, 100081, China.
E-mail addresses: tongjinliu@163.com (T. Liu), zhangyoujun@caas.cn (Y. Zhang), zhangxiaohui01@caas.cn (X. Zhang), syy1111@126.com (Y. Sun), wanghaiping@caas.cn (H. Wang), songjiangping@caas.cn (J. Song), lixixiang@caas.cn (X. Li).

https://doi.org/10.1016/j.plaphy.2019.04.006
Received 28 November 2018; Received in revised form 22 February 2019; Accepted 5 April 2019
Available online 11 April 2019
0981-9428/

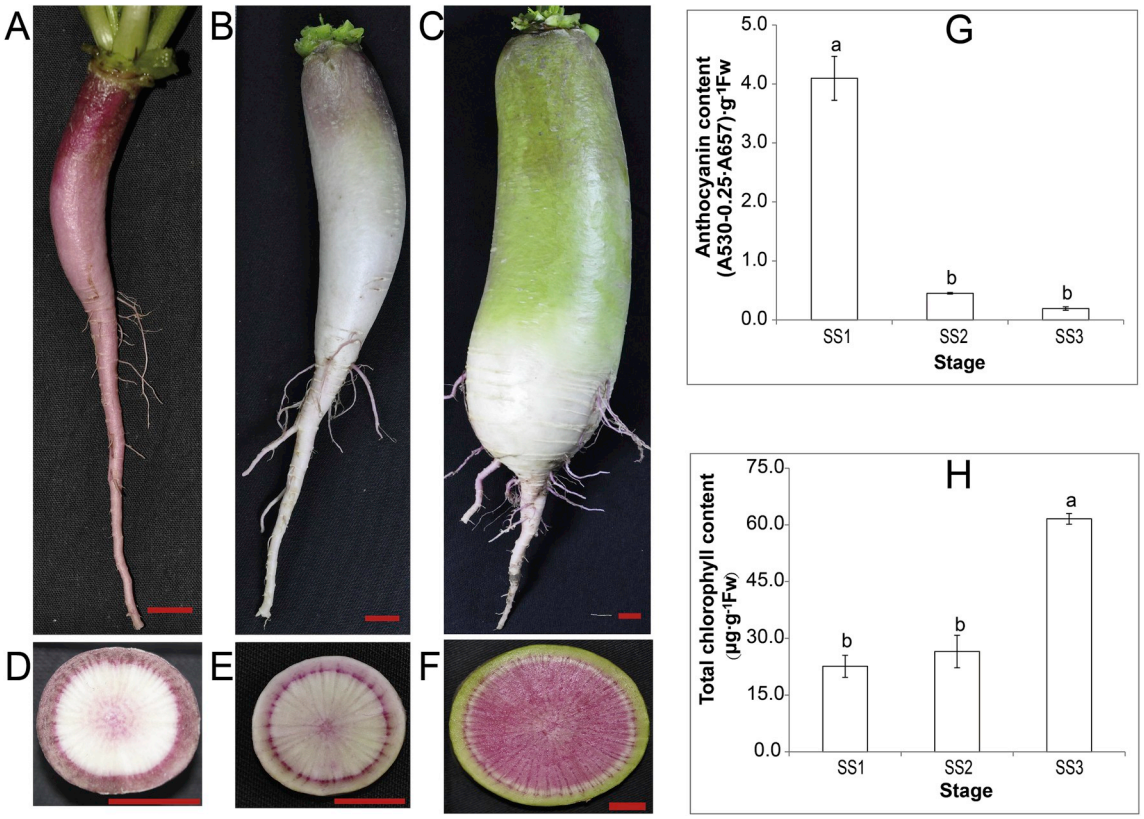

Fig. 1. Images of 'Xinlimei' radish taproots and pigment contents in the skin. (**A–C**) Photos of 'Xinlimei' radish taproots at three different developmental stages. (**D–F**) Images of 'Xinlimei' radish taproots at the above three stages; bars in **A-F** = 1 cm. (**G**) Relative total anthocyanin content of the skin of a 'Xinlimei' radish taproot. (**H**) Total chlorophyll content of the skin of a 'Xinlimei' radish taproot. Error bars show standard errors (SEs) of the means of anthocyanin and chlorophyll contents.

breakdown of chlorophyll and a substantial increase in anthocyanin content (Lai et al., 2015). Anthocyanins are synthesized through a branch of the flavonoid pathway, which has been extensively studied in many species (Park et al., 2011; Zhang et al., 2015; Chen et al., 2016; Cao et al., 2018). The most important transcription factor complexes regulating downstream genes encoding enzymes involved in anthocyanin biosynthesis are MBW complexes, consisting of MYB, basic helix-loop-helix and WD40 (Koes et al., 2005). Although most of the genes controlling anthocyanin biosynthesis in radish have been reported (Park et al., 2011; Chen et al., 2016; Muleke et al., 2017; Sun et al., 2018), to our knowledge, only two transcription factors (*RsMYB1* and *RsTT8*) have been reported as regulating anthocyanin accumulation in radish taproot (Lim et al., 2016, 2017; Yi et al., 2018). Anthocyanins are synthesized at the cytoplasmic surface of the endoplasmic reticulum and are then transported to vacuoles by members of the glutathione S-transferase (GST), ATP-binding cassette and multidrug and toxic compound extrusion (MATE) families (Koes et al., 2005; Klein et al., 2006; Gomez et al., 2009, 2011). In contrast to biosynthesis pathways, knowledge of anthocyanin catabolism in plants is limited (Oren-Shamir, 2009; Muleke et al., 2018). For example, polyphenol oxidases, β-glucosidases and class III peroxidases catalyze anthocyanin degradation in fruit juices, yet only one class III peroxidase, BcPrx01, has been shown to be responsible for in planta anthocyanin degradation (Oren-Shamir, 2009; Zipor et al., 2015).

As a photosynthetic pigment, chlorophyll is vital for plant growth, and its metabolic pathway is well characterized in many species. The pathway begins with glutamic acid as a substrate and includes three stages: chlorophyll biosynthesis, the chlorophyll cycle and chlorophyll degradation. At least 30 genes for all 17 steps of chlorophyll biosynthesis have been identified in *Arabidopsis* (Beale, 2005), and expression of these genes is positively or negatively regulated by transcription factors, including ANAC046, EIN3, ORE1, FLU, GLK1, GLK2, ARC3, ARC5, ARC6, PIF1, PIF3, GNC, and CGA1 (Fitter et al., 2002; Beale, 2005; Yasumura and Langdale, 2005; Adhikari et al., 2011; Abolhassani Rad et al., 2018; Majee et al., 2018). Overall, a dynamic balance between chlorophyll biosynthesis and degradation is important, and five genes involved in chlorophyll degradation have been reported: *CLH1*, *CLH2*, *PPH*, *PAO* and *RCCR* (Lai et al., 2015; Shimoda et al., 2016). Previous studies have shown that the stay green (SGR) protein, encoding Mg-dechelatase, is essential for the initiation of chlorophyll degradation (Lai et al., 2015; Shimoda et al., 2016). Although structural genes and transcription factors involved in chlorophyll metabolism have been well characterized in many plant, the metabolic pathway in radish remains largely unknown. Genome-wide identification and expression analysis of chlorophyll metabolic genes will not only be helpful for revealing the molecular mechanisms underlying 'Xinlimei' taproot skin greening but will also provide insight into the mechanisms involved in the formation of green flesh and/or green-skinned radish and a basis for further studies.

In this study, taproot skin samples from three distinct growth stages of 'Xinlimei' radish were used for RNA sequencing (RNA-Seq) to investigate the expression profiles of related genes. Focusing mainly on flavonoid and chlorophyll metabolism, global gene expression profiles during taproot development were analyzed. To the best of our knowledge, this is the first report of the identification of chlorophyll metabolic genes in radish at the genome-wide level and analysis of their expression, and critical genes associated with red skin fading and greening were identified. These results will be helpful for elucidating the mechanism responsible for the dynamic changes that occur in red fading and greening of 'Xinlimei' radish taproot skin and for improving appearance quality through molecular design breeding and agricultural production techniques. The chlorophyll metabolic genes identified in

the present study also provide a basis for further research on the mechanisms of green flesh and/or green-skin radish formation.

2. Materials and methods

2.1. Plant materials

Seeds of the advanced inbred line 'CCHX17-6-12' of 'Xinlimei' radish were sown in a plastic tunnel in 2017 at The Institute of Vegetables and Flowers (IVF), Chinese Academy of Agricultural Sciences (CAAS), Beijing, China. The taproots were harvested at 30, 38 and 66 d after sowing because their epidermis (skin) shows distinct colors at these three development stages, red, white and green, respectively (Fig. 1). The skin of the taproot was manually peeled and cut into small cubes, and the samples were frozen in liquid nitrogen and stored at −80 °C for further study.

2.2. Total anthocyanin and chlorophyll content measurements

Total anthocyanins were extracted from 0.5 g of finely ground taproot skin and evaluated by measuring absorbance of the extract at 530 and 657 nm, as described previously (Chu et al., 2013). Chlorophyll was extracted with 80% acetone for 24 h in the dark and assessed by measuring the absorbance at 663 and 645 nm, as described by Liu et al. (2014). All samples were evaluated in triplicate in three independent biological replicates.

2.3. Strand-specific RNA-Seq library construction and illumina sequencing

Total RNA was extracted and purified from radish taproot skin frozen in liquid nitrogen using an RNAprep Pure Plant Kit (TIANGEN, Beijing, China) according to the manufacturer's instructions. Three biological replicates were used for each sample. The quality of RNA was examined using a NanoDrop Spectrophotometer (NanoDrop 2000C, Wilmington, DE, USA), agarose gel electrophoresis and an Agilent 2100 Bioanalyzer (Agilent Technologies, Santa Clara, CA, USA). A total of 10 μg qualified RNA was used for RNA-Seq library construction. mRNA was isolated using oligo (dT)-magnetic beads and then fragmented, and first-strand cDNA was synthesized using random hexamer primers. Second-strand cDNA was synthesized using buffer, dNTPs (dUTP was used instead of dTTP), RNase H and DNA polymerase I. End repair and 3′-end single-nucleotide A (adenine) addition were performed, and sequencing adaptors were ligated to the fragments. The fragments were chosen based on size, and the cDNA was digested with the USER enzyme to produce the final sequencing information for the first-strand cDNA. Fragments were enriched by PCR amplification, and the amplified products were purified using AMPure XP beads to produce strand-specific cDNA libraries, which were sequenced using an Illumina HiSeqTM XTEN (San Diego, CA, USA) system at Mega Genomics (Beijing, China).

2.4. RNA-seq analysis

Before analysis, various quality control measures for the Fastq files of raw sequence data were performed using NGS QC Toolkit (Patel and Jain, 2012), including removal of adaptors from the raw reads and removal of reads with more than 10% unknown bases as well as low-quality reads (having more than 50% bases with a quality value ≤ 5). The clean reads were aligned to radish genome 'XYB36-2' (Zhang et al., 2015) using the SOAP aligner/SOAP2 program, with less than five-nucleotide mismatch allowed (Li et al., 2009). The level of gene expression was determined based on the fragments per kilobase of transcript per million mapped reads (Mortazavi et al., 2008). Statistical comparisons between the samples were performed using DEGSeq R package (1.12.0) (Wang et al., 2009). The false discovery rate (FDR) was employed to determine the threshold *P* value in multiple comparisons. Differentially expressed genes (DEGs) were considered those with FDR values < 0.001 and absolute values of $\log_2$ (fold change) ≥ 1.

2.5. Anthocyanin and chlorophyll metabolism gene identification in radish

Protein sequences representing the complete set of anthocyanin and chlorophyll metabolism genes in *Arabidopsis thaliana* were acquired from TAIR (www.arabidopsis.org). The database used for radish protein sequences was obtained from a previous whole-genome sequencing project (Zhang et al., 2015). We identified candidate genes related to anthocyanin and chlorophyll metabolism in radish using BLASTP with a cutoff E-value ≤ 1E-10. To exclude mismatches, the resulting radish sequences were manually searched for the best matches in the Araport11 protein sequence database using BLAST tools in TAIR, and only the best matching homologs were designated as orthologous genes.

2.6. Phylogenetic tree and sequence alignment

Amino acid sequences of MYB and bHLH transcription factors were acquired from the NCBI non-redundant protein (Nr) database (http://www.ncbi.nlm.nih.gov) and aligned. A phylogenetic tree was generated using MEGA 5.05 (Tamura et al., 2011) using the neighbor-joining method with 1000 bootstrap replicates. Sequence alignment was performed using DNAMAN version 8 (Lynnon, Quebec, Canada) with default parameters.

2.7. Quantitative real-time PCR (qPCR) validation

To verify the reliability of the RNA-Seq results, twelve genes related to anthocyanin and chlorophyll metabolism were selected for qPCR analysis. 800 ng of total RNA was reverse transcribed to synthesize first-strand cDNA using oligod primers and *EasyScript*® One-Step gDNA Removal and cDNA Synthesis Super Mix (TransGen Biotech, China) and diluted 20-fold as templates for qPCR. qPCR was performed using a StepOne™ Real-Time PCR System (Applied Biosystems), with the *TransStart*® Green qPCR SuperMix (TransGen Biotech) and our previously employed reaction conditions in a 20-μL volume (Liu et al., 2016). A list of genes and primers is shown in Table S1. Three independent biological and technical replicates were performed. Data were analyzed using StepOne™ Softwarev.2.0 (Applied Biosystems). The radish *GADPH* gene was utilized as an internal control, and relative expression levels were estimated using the $2^{-\Delta\Delta CT}$ method (Livak and Schmittgen, 2001).

2.8. Statistical analyses

SPSS 17.0 and the Microsoft Excel 2007 package for Windows were applied for statistical analyses. Data were analyzed for significant differences using Tukey's HSD test at a significance threshold of $p = 0.05$. Heat maps were prepared using HemI 1.0 software (Deng et al., 2014).

3. Results

3.1. Chlorophyll and anthocyanin contents in 'Xinlimei' radish taproot skins at three developmental stages

The red color of the taproot skin of 'Xinlimei' radish appeared at developmental stage 1 [SS1, 30 d after sowing (DAS); Fig. 1A and D], gradually faded to white at developmental stage 2 (SS2, 38 DAS; Fig. 1B and E), and turned green at developmental stage 3 (SS3, 66 DAS; Fig. 1C and F). These phenotypic changes in taproot skin color coincided with changes in anthocyanin and chlorophyll contents (Fig. 1Gand H). The taproot skin exhibited the highest anthocyanin content at SS1, which sharply decreased at SS2; however, there was no significant difference between SS2 and SS3 (Fig. 1G). Chlorophyll

Table 1
RNA-sequencing and sample transcriptome mapping.

Sample name	Clean Reads	Mapped Reads	Uniquely Mapped Reads	Multiple Map Reads	Reads Map to '+'	Reads Map to '-'
SS1-1	47,931,412	34,904,473 (72.82%)	33,054,608 (68.96%)	1,849,865 (3.86%)	16,924,249 (35.31%)	16,954,003 (35.37%)
SS1-2	49,525,134	35,355,198 (71.39%)	33,595,354 (67.83%)	1,759,844 (3.55%)	17,186,912 (34.70%)	17,252,320 (34.84%)
SS1-3	48,953,322	35,341,444 (72.19%)	33,554,270 (68.54%)	1,787,174 (3.65%)	17,180,369 (35.10%)	17,205,465 (35.15%)
SS2-1	49,175,148	35,978,251 (73.16%)	34,198,655 (69.54%)	1,779,596 (3.62%)	17,486,760 (35.56%)	17,527,227 (35.64%)
SS2-2	49,422,694	36,117,101 (73.08%)	34,369,652 (69.54%)	1,747,449 (3.54%)	17,573,274 (35.56%)	17,617,392 (35.65%)
SS2-3	49,319,484	35,953,932 (72.90%)	34,308,851 (69.56%)	1,645,081 (3.34%)	17,535,325 (35.55%)	17,578,624 (35.64%)
SS3-1	46,876,122	32,870,176 (70.12%)	31,636,862 (67.49%)	1,233,314 (2.63%)	16,136,804 (34.42%)	16,149,727 (34.45%)
SS3-2	49,170,384	34,464,541 (70.09%)	33,059,894 (67.24%)	1,404,647 (2.86%)	16,885,712 (34.34%)	16,934,056 (34.44%)
SS3-3	48,994,278	34,860,867 (71.15%)	33,543,809 (68.46%)	1,317,058 (2.69%)	17,114,161 (34.93%)	17,139,344 (34.98%)

contents between SS1 and SS2 were not significantly but were significantly lower than during SS3 (Fig. 1H).

3.2. RNA-seq data analysis

For the SS1, SS2 and SS3 libraries, averages of 48,803,289, 49,305,775 and 48,346,928 clean reads, respectively, were produced by RNA-Seq (Table 1). In total, 70.09%–73.16% and 67.24%–68.96% of the clean reads were mapped and uniquely mapped, respectively, to reference genome 'XYB36-2' (Zhang et al., 2015), with 34.34%–35.31% and 34.44%–35.37% of the clean reads mapped to the '+' and '−' strands, respectively (Table 1). Accordingly, the RNA-Seq data obtained were sufficient for further analyses.

3.3. Identification of DEGs

To predict candidate genes responsible for 'Xinlimei' taproot skin color fading, DEGs were identified by pairwise comparisons of expression levels at the three developmental stages (Fig. 2). A total of 3600 (1725 upregulated and 1875 downregulated), 2721 (1367 upregulated and 1354 downregulated) and 5679 (2677 upregulated and 3002 downregulated) DEGs were identified in three comparison groups, SS1 vs SS2, SS2 vs SS3 and SS1 vs SS3, respectively (Fig. 2A and B), and these genes were selected as candidate genes potentially involved in taproot skin color fading. Additionally, Venn diagram analysis showed that 488 genes of the DEGs were significantly differentially expressed among all pair-wise comparisons (Fig. 2B).

Kyoto Encyclopedia of Genes and Genomes enrichment analysis was conducted to identify pathway-related DEGs, and 'photosynthesis', 'phenylpropanoid biosynthesis', 'starch and sucrose metabolism', 'photosynthesis–antenna proteins', 'phenylalanine metabolism' and 'glutathione metabolism' were all enriched in the three comparison groups (Fig. 3). In addition, pathways of 'carbon fixation in photosynthetic organisms', 'flavonoid biosynthesis', 'carbon metabolism', 'pentose phosphate pathway' and 'stilbenoid, diarylheptanoid and gingerol biosynthesis' were significantly different between the stages in which skin color varied (SS1 vs SS2 and SS1 vs SS3), whereas no changes were observed between the two stages after color fading (SS2 vs SS3) (Fig. 3). Furthermore, significant enrichment of DEGs in the 'porphyrin and chlorophyll metabolism' pathway was found; therefore, this pathway most likely contributes to the greening process of 'Xinlimei' radish taproot skin. Notably, all DEGs involved in 'photosynthesis' and 'photosynthesis-antenna proteins' pathways were significantly upregulated (Fig. S3).

3.4. Genes involved in anthocyanin synthesis, degradation and transport

Anthocyanin biosynthesis is a well-studied pathway in plants, and related genes in radish have been identified (Muleke et al., 2017; Naoumkina et al., 2010; Sun et al., 2018). In the present study, the expression levels of these genes in 'Xinlimei' taproot skins were compared among the developmental stages (Fig. 4). Regarding genes encoding phenylalanine ammonia-lyase and cinnamate-4-hydroxylase, which catalyze the initial two steps of anthocyanin biosynthesis, no significant differences in expression among SS1, SS2 and SS3 were found (Fig. 4, Table S2). In contrast, two predicted chalcone synthase-encoding genes (*Rsa10002061* and *Rsa10025178*) were significantly downregulated at SS2 and SS3 compared with SS1, and a predicted chalcone synthase-encoding gene (*Rsa10036148*) was significantly downregulated at SS3 compared with SS1 and SS2 (Fig. 4, Table S2). Furthermore, one predicted 4-coumarate: CoA ligase-encoding gene (*Rsa10033870*), one predicted chalcone isomerase-encoding gene (*Rsa10028242*), flavanone 3-

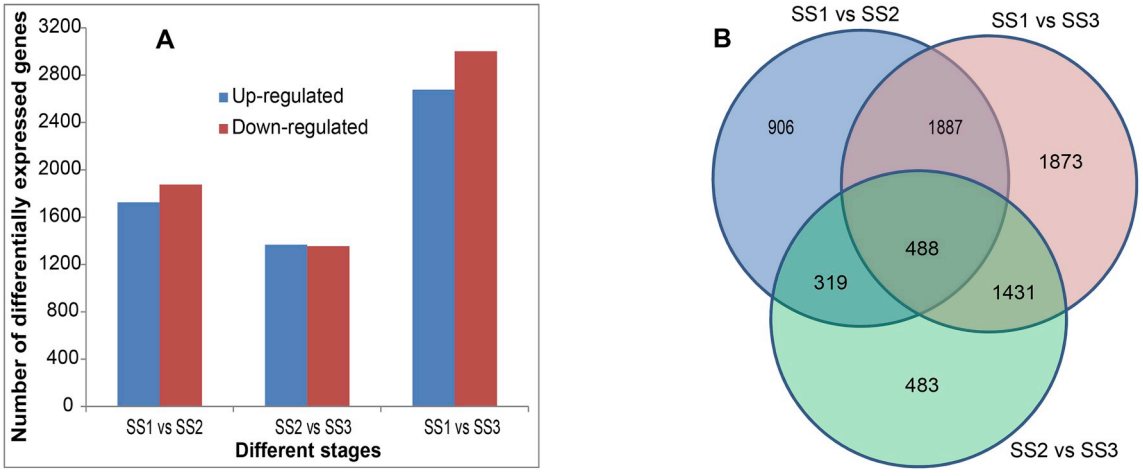

Fig. 2. Distribution of differentially expressed genes (DEGs) based on the three stages of 'Xinlimei' radish taproot skin color changes. (**A**) The numbers of up- and down-regulated DEGs; (**B**) Venn diagram illustrating the number of DEGs revealed by pairwise comparisons. (For interpretation of the references to color in this figure legend, the reader is referred to the Web version of this article.)

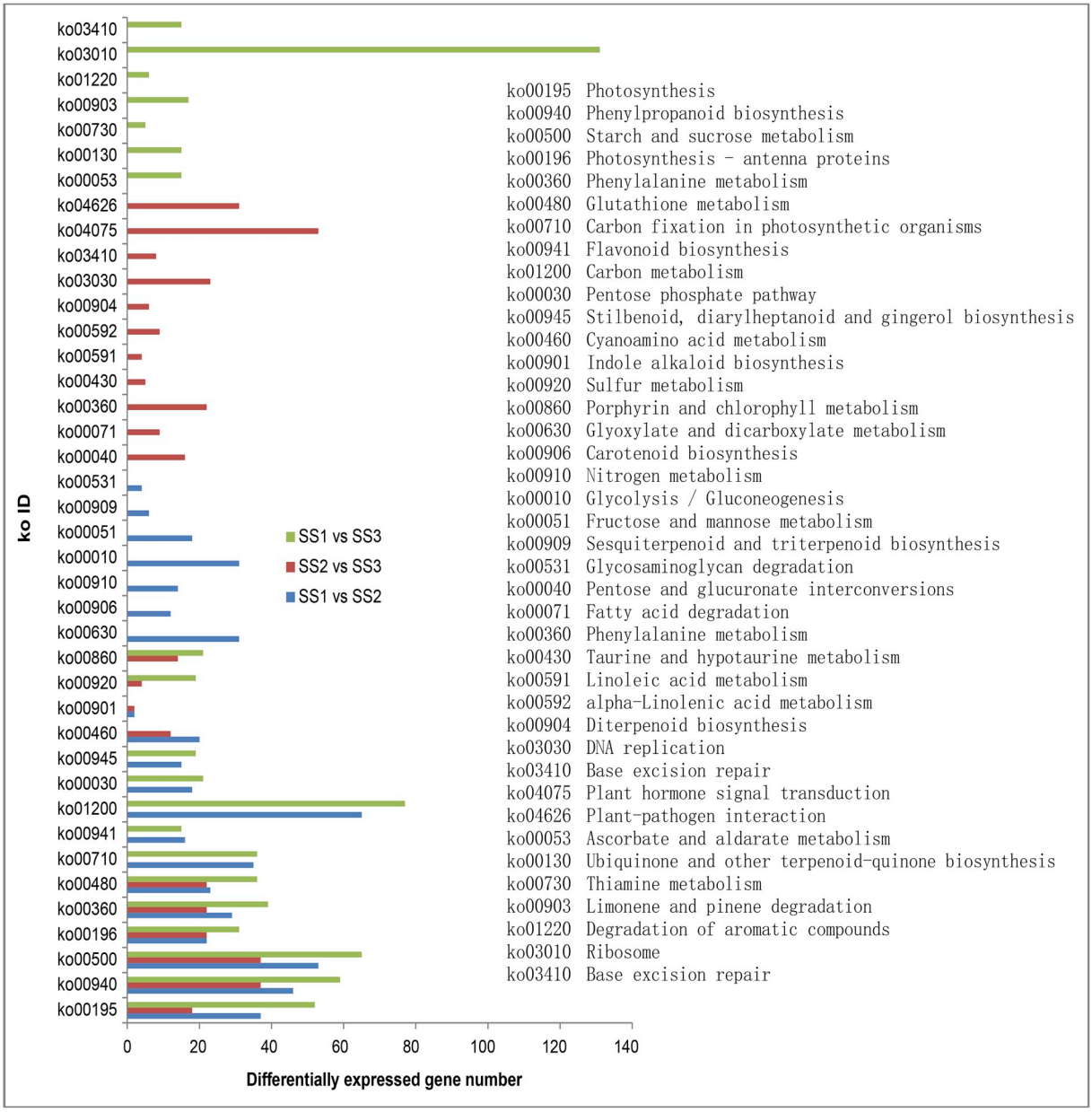

Fig. 3. KEGG (Kyoto Encyclopedia of Genes and Genomes) pathway enrichment of DEGs.

hydroxylase-encoding gene (*Rsa10032967*), dihydroflavonol-4-reductase-encoding gene (*Rsa10008592*), anthocyanidin synthase-encoding gene (*Rsa10014262*) and three predicted glucuronosyltransferase-encoding genes (*Rsa10003826*, *Rsa10018705* and *Rsa10027999*) were significantly down-regulated in SS2 and SS3 compared with SS1 (Fig. 4, Table S2). Although three copies (*Rsa10013517*, *Rsa10042069* and *Rsa10042068*) of the flavonol synthase (FLS)-encoding gene are present in the genome, the latter two were not detected in 'Xinlimei' radish taproot skin at any of the three stages (Fig. 4B); *Rsa10013517* was significantly downregulated at SS1 and SS3 compared with SS2 but was not associated with anthocyanin degradation (Fig. 1G).

Anthocyanins are synthesized in the cytosol, and the colors are displayed after transport to and accumulation in vacuoles (Winkel-Shirley, 2001). In the present study, two genes (*Rsa10018713* and *Rsa10015104*) were identified as homologs of *transparent testa 19* (*AtTT19*), which encodes an *A. thaliana* GST that functions as a carrier transporting anthocyanins from the cytosol to the tonoplast (Sun et al., 2012). The homologous gene in *Litchi*, *GST4*, complements the anthocyanin-less phenotype of the *tt19* mutant (Hu et al., 2016). The expression levels of *Rsa10018713* and *Rsa10015104* were significantly down-regulated in SS2 and SS3 compared with SS1 (Fig. 4, Table S2). However, because the expression level of *Rsa10018713* was significantly greater than that of *Rsa10015104* (46.4-fold), the former is a more likely candidate anthocyanin transporter gene.

Peroxidase is involved in anthocyanin degradation (Zipor et al., 2015) and in the present study, 132 predicted peroxidase-encoding genes were identified based on functional annotation (Table S3). For *Rsa10017424*, expression levels in SS2 and SS3 were greater than those in SS1, indicating that this gene may be involved in anthocyanin degradation in 'Xinlimei' radish taproot skin.

3.5. Transcription factors involved in anthocyanin biosynthesis regulation

Expression of anthocyanin biosynthetic genes is regulated by a series of transcription factors, with the MBW complex being the most important, and we identified 68 MYB-encoding genes among the DEGs

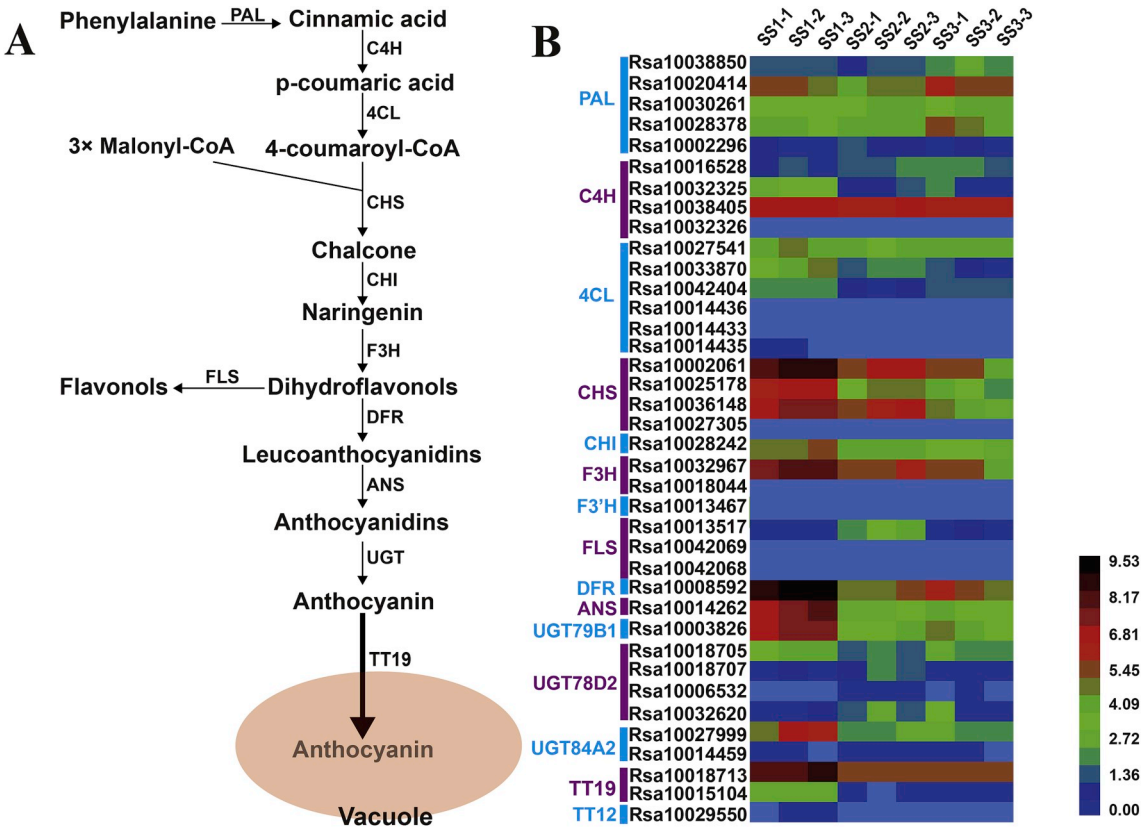

Fig. 4. Anthocyanin biosynthesis pathway and gene expression in 'Xinlimei' radish taproot skin. (**A**) The anthocyanin biosynthesis pathway adopted from *Arabidopsis thaliana*. (**B**) Expression pattern of genes involved in anthocyanin synthesis and transport. PAL, phenylalanine ammonia-lyase; C4H, Cinnamate-4-hydroxylase; 4CL, 4-coumarate:CoA ligase; CHS, chalcone synthase; CHI, chalcone isomerase; F3H, flavanone 3-hydroxylase; F3′H, flavonoid 3′-hydroxylase; FLS, flavonol synthase; DFR, dihydroflavonol-4-reductase; ANS, anthocyanidin synthase; UGT, glucuronosyltransferase; TT19, transparent testa 19; TT12, transparent testa 12.

(Table S4). Phylogenetic analysis of these candidate MYBs was then conducted with *A. thaliana* MYBs involved in anthocyanin biosynthesis as well as previously published radish RsMYB1 (Fig. 5A). The AtMYBs grouped into two anthocyanin biosynthesis-regulated clades: one including AtMYB11, AtMYB12, AtMYB111 and radish Rsa10009916, and another including AtMYB75, AtMYB90, AtMYB114 and radish RsMYB1, Rsa10033919, Rsa10034073, Rsa10008423. Among them, the expression levels of *Rsa10009916* and *Rsa10034073* were significantly higher in SS2 than in SS1 and SS3 (Fig. 5B). Considering that the expression trend of *Rsa10009916* and *Rsa10034073* differed from that of structural anthocyanin biosynthesis genes in radish, these two genes are not likely involved in anthocyanin biosynthesis regulation. Additionally, *Rsa10008423* exhibited low expression in SS1 and SS2, with no significant difference between these two stages (Fig. 5B), indicating that this gene likely does not participate in anthocyanin biosynthesis regulation in radish taproot skin. The expression level of *Rsa10033919* was reduced in SS2 and SS3 compared with SS1 (Fig. 5B), with similar expression trends with structural genes (Fig. 4B), and sequence alignment of the deduced amino acid sequences (Fig. 5C) indicated that it is the same gene as previously reported *RsMYB1* (Lim et al., 2016). Therefore, *Rsa10033919*, designated *RsMYB1*, is likely involved in regulating anthocyanin biosynthesis in the taproot skin of 'Xinlimei' radish.

Forty-three bHLH encoding genes were also identified (Table S5). Our phylogenetic analysis using deduced amino acid sequences showed that Rsa10033334 and Rsa10029348 grouped into an anthocyanin biosynthesis-related bHLH clade that included *A. thaliana* AtEGL3, AtGL3, AtTT8, *Litchi chinensis* LcbHLH1, and *Raphanus sativus* RsTT8 (Fig. 6A). Based on previous studies, AtTT8, AtEGL3 and AtGL3 have partially redundant functions in anthocyanin biosynthesis (Hichri et al., 2011). Thus, we speculate that Rsa10033334 and Rsa10029348 might be functionally redundant with regard to anthocyanin biosynthesis in the skin of radish taproot. The expression trend of *Rsa10029348* exhibited significant downregulation in SS2 and SS3 compared with SS1 (Fig. 6B), with expression trends similar to those of structural genes (Fig. 4B). The above results indicate that Rsa10029348, designated as RsTT8, is most likely involved in regulating anthocyanin biosynthesis in 'Xinlimei' radish taproot skin.

Functional annotation revealed 29 candidate WD40 genes in the 'Xinlimei' radish taproot skin transcriptome (Table S6). However, significantly different expression among SS1, SS2 and SS3 was not found for any of these genes, including *Rsa10018278*, a homolog of *A. thaliana transparent testa glabra 1* (*AtTTG1*), which functions in regulating anthocyanin accumulation (Gonzalez et al., 2008). Thus, *RsMYB1* and *RsTT8*, but not *WD40*, play major roles in regulating color fading in 'Xinlimei' radish taproot skin.

3.6. Expression patterns of genes involved in chlorophyll metabolism

The chlorophyll metabolism pathway has been well identified and characterized in the leaves of higher plants, though to the best of our knowledge, the genes involved in these processes in radish have not yet been reported. The taproot skin of 'Xinlimei' radish turns green from red as it matures, and to confirm crucial players in the greening process, we identified genes involved in chlorophyll metabolism on a genome-wide level and compared their expression patterns among three developmental stages. The chlorophyll metabolism pathway is generally divided into three stages: chlorophyll biosynthesis, the chlorophyll cycle and chlorophyll degradation. In the present study, 73 genes in radish were identified as orthologs of 49 chlorophyll metabolism genes in *A. thaliana*. Moreover, chlorophyll metabolism genes have expanded in radish, and 42.9% of these genes are present in more than one copy, with more biosynthesis and cycle genes retained than degradation

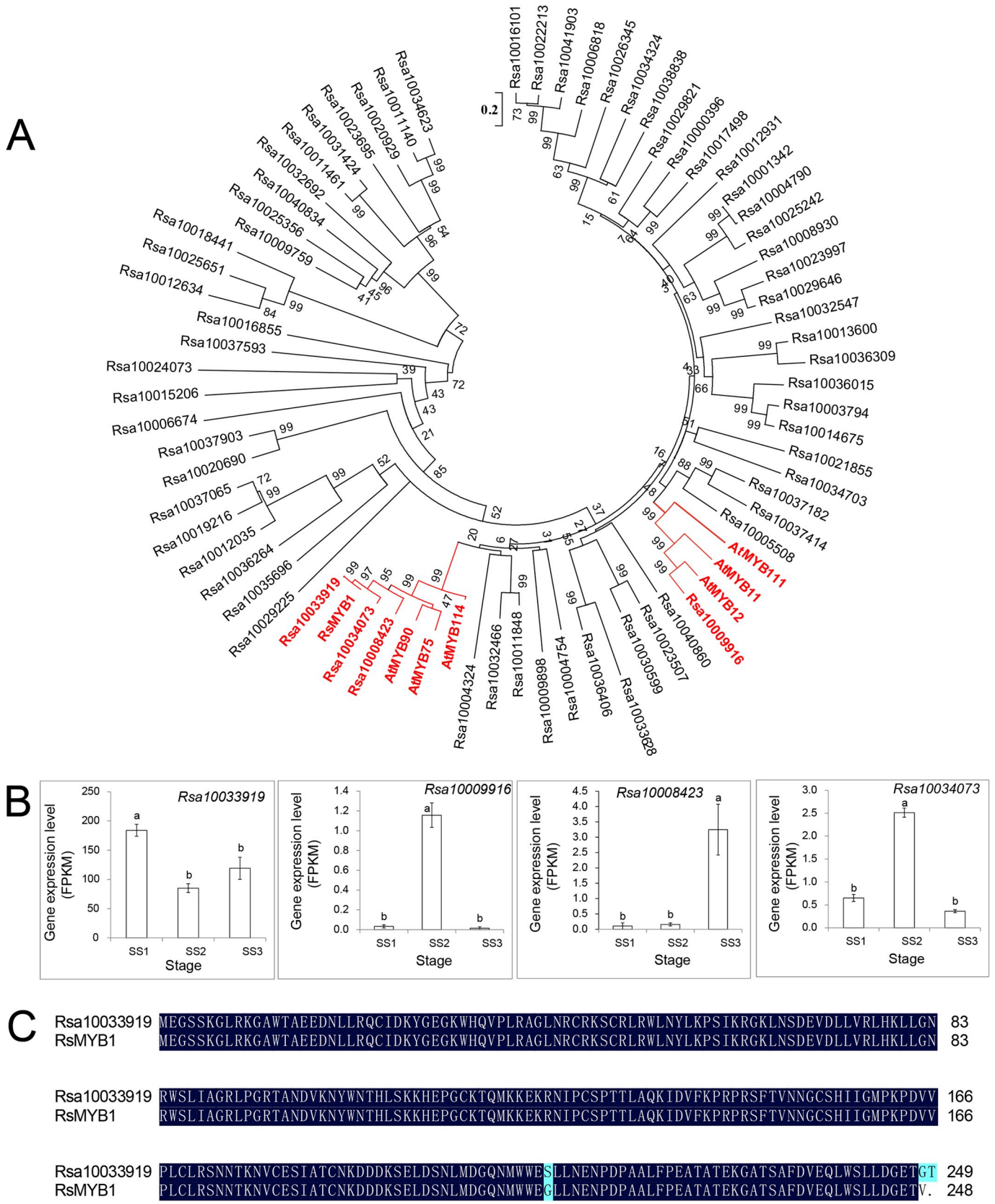

Fig. 5. Identification of MYBs involved in regulating anthocyanin biosynthesis in radish. (**A**) Phylogenetic relationships among putative MYBs in radish and anthocyanin MYB regulators in *Arabidopsis thaliana*. The numbers next to nodes are bootstrap values from 1000 replications. The red clade comprises putative anthocyanin-regulating MYBs. GenBank accession numbers are as follows: AtMYB11 (NP_191820), AtMYB12 (NP_182268.1), AtMYB75 (NP_176057.1), AtMYB90 (NM_105310), AtMYB111 (NP_199744), AtMYB114 (NP_176812), RsMYB1 (AKM95888.1). (**B**) Expression levels of candidate anthocyanin-regulating MYBs in 'Xinlimei' radish based on RNA-sequencing data. Error bars indicate the SE of three biological replicates. (**C**) Sequence alignment of the deduced amino acid sequences of Rsa10033919 and RsMYB1. (For interpretation of the references to color in this figure legend, the reader is referred to the Web version of this article.)

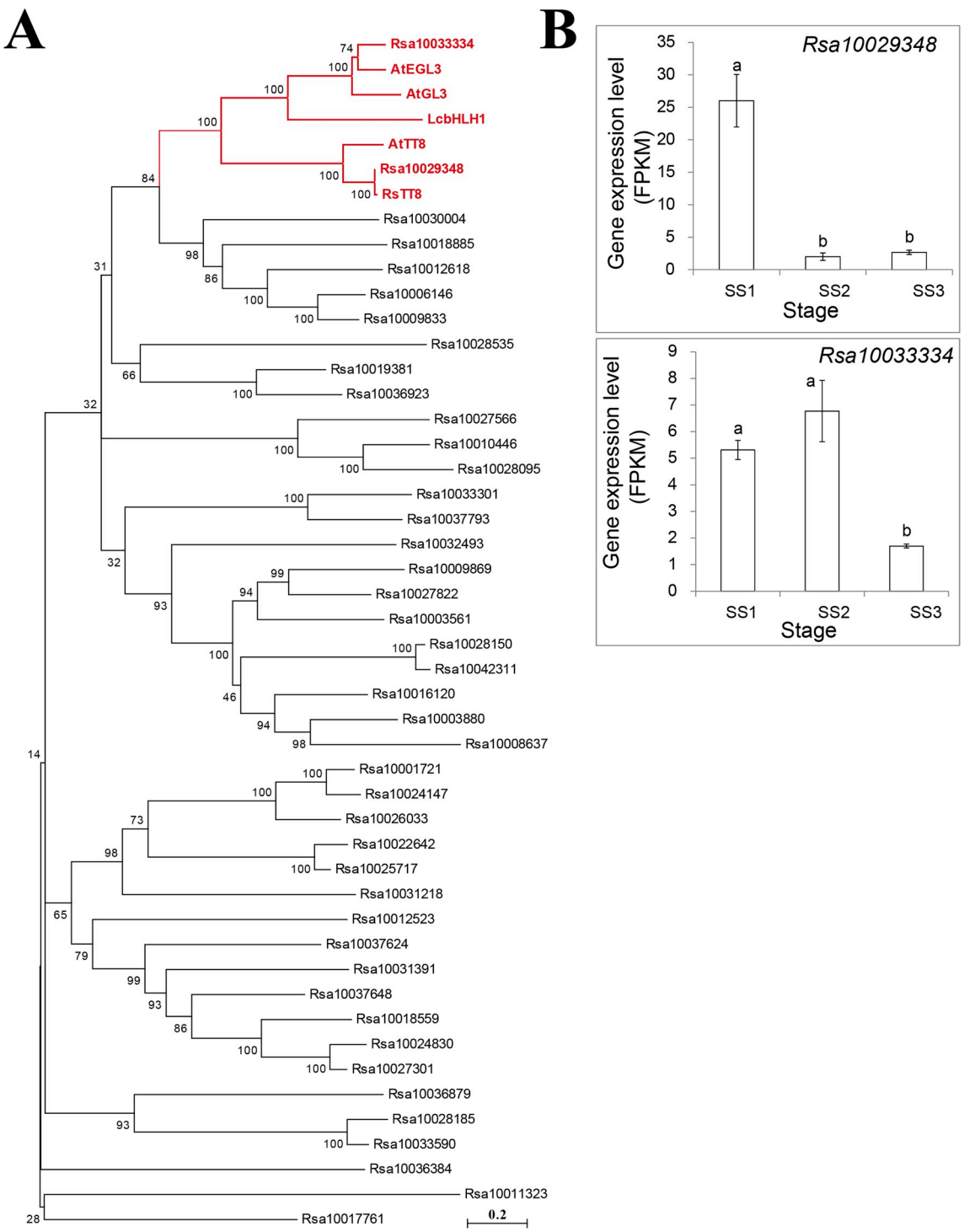

Fig. 6. Identification of bHLHs involved in regulating anthocyanin biosynthesis in radish. (**A**) Phylogenetic relationships among putative bHLHs in radish and anthocyanin bHLH regulators in other species. The numbers next to nodes are bootstrap values from 100 replications. The red clade comprises putative anthocyanin-regulating MYBs. GenBank accession numbers are as follows: AtEGL3 (NP 176552), AtGL3 (NP680372), HcbHLH1 (APP94122.1), AtTT8 (Q9FT81), and RsTT8 (ASF79354.1). (**B**) Expression levels of candidate anthocyanin-regulating bHLHs in 'Xinlimei' radish based on RNA-sequencing data. Error bars indicate the SE of three biological replicates. (For interpretation of the references to color in this figure legend, the reader is referred to the Web version of this article.)

genes (Fig. 7, Table S7).

GluRS catalyzes the first step of the chlorophyll biosynthetic pathway, and although two copies were identified in the 'XYB36-2' genome, neither showed significant differences among the three developmental stages (30, 38 and 66 days after sowing) in 'Xinlimei' radish taproot skin (Fig. 7, Table S7). In addition, two copies of *GSA1*, and one each of *HEMB1*, *HEMB2*, *HEMD*, *HEME1*, *HEME2*, *HEMF1*, *PORA* and *DVR* are present in the radish genome, though with no significant differences among the three developmental stages. In contrast, two *HEMA1*, four *HEMA2*, one *HEMG1*, two *HEMG2*, one *CHLH*, one *CHLD*, two *CHLI1*, one *CHLI2*, one *CHLM*, two *CRD1*, one *PORB*, two *PORC*, and two *CHLG* copies were found in the radish genome, and at least one copy of each gene was significantly upregulated in the greening process of 'Xinlimei' radish taproot skin. There are four genes

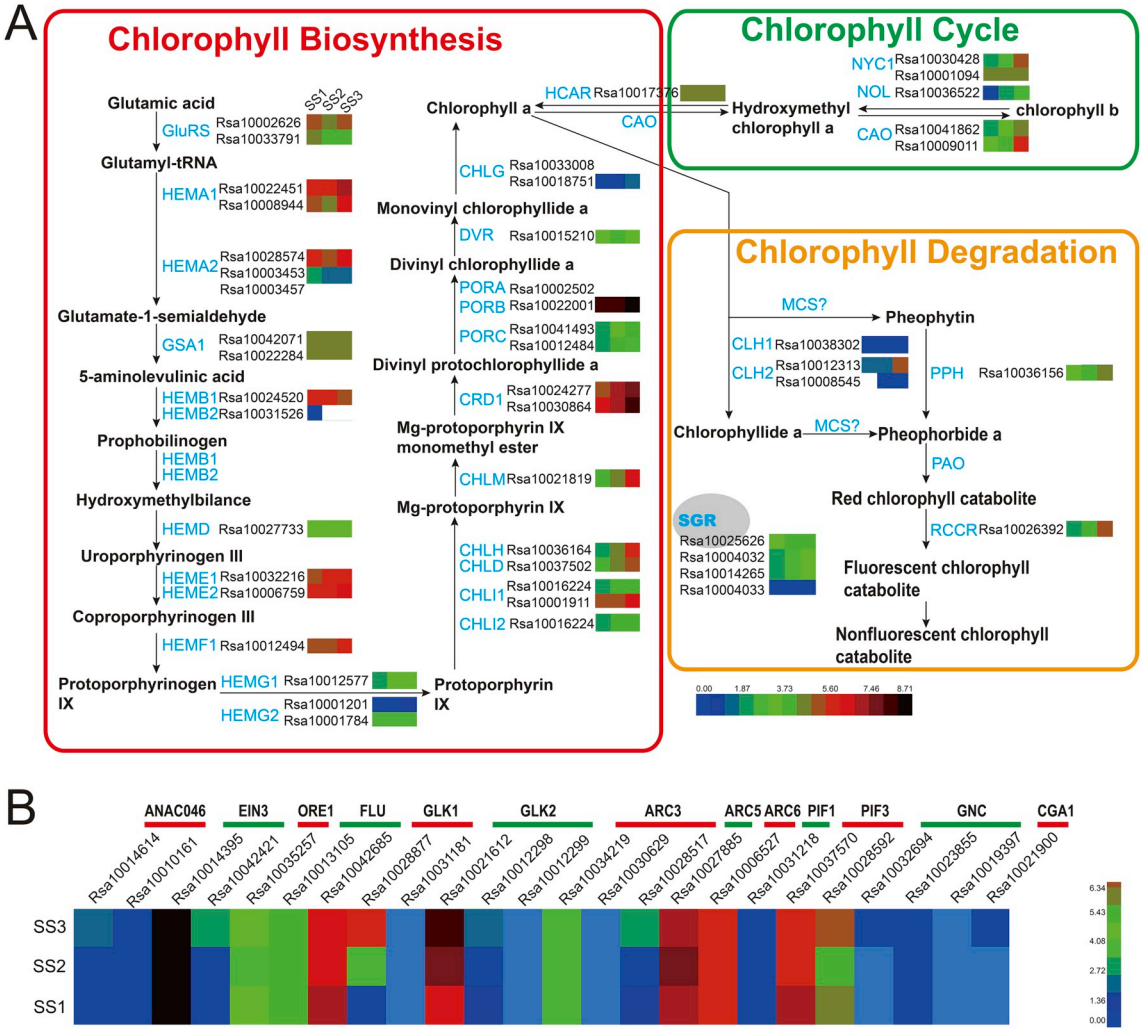

Fig. 7. Radish genes that might be involved in chlorophyll metabolism and their expression levels. The heatmap presents the $\log_2$ values (FPKM) of chlorophyll metabolism genes based on RNA-sequencing data at 30, 38 and 66 days after sowing. GluRS, glutamyl–tRNA synthetase; HEAM, glutamyl tRNA reductase; GSA (HEML), glutamate 1-semialdehyde aminotransferase; HEMB, 5-aminolevulinate dehydratase; HEMD, uroporphyrinogen III synthsae; HEME, uroporphyrinogen decarboxylase; HEMF, coproporphyrinogen oxidative decarboxylase; HEMG, protoporphyrinogen oxidase; CHLH, Mg chelatase H subunit; CHLD, Mg chelatase D subunit; CHLI, Mg chelatase I subunit; CHLM, Mg-protoporphyrin IX methyltransferase; CRD1 (ACSF), Mg-protoporphyrinogen IX monomethylester cyclase; PORA, protochlorophyllide oxidoreductase A; PORB, protochlorophyllide oxidoreductase B; PORC, protochlorophyllide oxidoreductase C; DVR, divinyl reductase; CHLG, chlorophyll synthase; CAO, chlorophyllide a oxygenase; HCAR, hydroxy-chlorophyll a reductase; NYC1, non-yellow coloring 1; NOL, NYC1-like; CLH, chlorophyllase; PPH, pheophytinase; PAO, pheide a oxygenase; RCCR, red chlorophyll catabolite reductase; SGR, chlorophyll; ANAC046, NAC domain containing protein 46; EIN3, ethylene insensitive 3; ORE1, ORESARA 1; FLU, thylakoid membrane protein FLUORESCENT; GLK, Golden2-like; ARC, accumulation and replication of chloroplast 5; PIF, PHY-interacting factor; GNC, GATA nitrate-inducible carbon-metabolism-involved; CGA1, cytokinin-responsive GATA factor 1. (For interpretation of the references to color in this figure legend, the reader is referred to the Web version of this article.)

involved in the chlorophyll cycle stage, and we identified one copy of *HCAR*, two of *CAO*, two of *NYC1* and one of *NOL* in the radish genome. Expression of these four genes was significantly enhanced in the greening process, indicating that the chlorophyll cycle stage might have an important role in this process. With regard to the chlorophyll degradation stage, one *CLH1*, two *CLH2*, one *PPH* and one *RCCR* copies were identified; except for *PPH*, the expression level of the other genes was similar, with the lowest expression at the red stage, moderate expression at the white stage, and highest expression at the green stage. It is noteworthy that the *PAO* gene was not found in the 'XYB36-2' genome, even though one copy has been identified in the WK10039 genome (Jeong et al., 2016).

SGR is involved in chlorophyll degradation, and four copies of this gene were found in the radish genome, two of which were significantly upregulated in the greening process. In addition, 13 transcription factors involved in regulating chlorophyll biosynthesis were identified and analyzed in the present study (Fig. 7B). Only one copy for *ORE1*, *ACR5*, *ACR6*, *PIF1* and *CGA1* was identified and two for *ANAC046*, *EIN3*, *FLU*, *GLK1*, *PIF3*; three copies of *GLK2*, *ARC3* and *GNC* were found. Among these transcription factors, *ANAC046*, *ORE1*, *ARC3*, *PIF1*, *GNC* and *CGA1* do not likely play important roles in regulating chlorophyll biosynthesis because of their very low expression levels, with FPKM values less than 7.85. In addition, *EIN3*, *FLU*, *GLK2*, *ARC5*, *ARC6* and *PIF3* showed no significant differences among the three different stages in the skin of the 'Xinlimei' radish and, were excluded as candidate genes involved chlorophyll biosynthesis regulation. Conversely, the expression levels of *GLK1* (*Rsa10028877*) at SS3 were 22- and 5-fold higher than those at SS1 and SS2, respectively. A previous report indicated that *Arabidopsis GLK1* and *GLK2* genes are functionally redundant in regulating chloroplast development (Fitter et al., 2002). Therefore, *Rsa10028877*, named after *RsGLK1*, is most likely the key candidate gene involved in regulating chlorophyll biosynthesis in 'Xinlimei' radish taproot skin.

To verify the reliability of the RNA-Seq data, six candidate genes

involved in anthocyanin metabolism (Fig. S2 A-F) and chlorophyll metabolism (Fig. S2 G-L) were selected for RT-qPCR assays. The results of these assays were consistent with those of the transcriptome analysis (Fig. S2 G-L).

4. Discussion

Taproot skin color is an important appearance quality trait in radish. Previous studies have shown that red-skinned radish largely occurs due to anthocyanin accumulation, mainly pelargonidin (Yi et al., 2018). In our present study, the skin of 'Xinlimei' taproot exhibited high anthocyanin and low chlorophyll contents at SS1 (Fig. 1). The red skin of 'Xinlimei' gradually fades to white during growth, with a sharp decrease in anthocyanin content according to our results. The findings are in agreement with those of Wang et al. (2017a,b), who found that a reduction in anthocyanin content results in fading of the red color of 'Red Bartlett' pears (*Pyrus communis* L.). Maturation processes in 'Xinlimei' radish were accompanied by skin greening, which was caused by chlorophyll accumulation (Fig. 1). However, the reverse process has been reported for the *Litchi* pericarp, in which degreening occurs during maturation because the chlorophyll content decreases and the anthocyanin content increases (Lai et al., 2015). These results indicate that the red color fading and greening of the taproot skin of 'Xinlimei' radish is induced by decreasing anthocyanin and increasing chlorophyll levels.

In the present study, DEGs identified by RNA-Seq were utilized for KEGG enrichment analysis. Three of the enriched pathways, 'phenylpropanoid biosynthesis', 'phenylalanine metabolism' and 'flavonoid biosynthesis', are related to anthocyanin biosynthesis, and downregulation of these pathways most likely contributes to the decrease in anthocyanin content detected during the red color-fading process of 'Xinlimei' radish taproot skin (Fig. 1). This result is in agreement with those of Wang et al. (2017a,b) and Lai et al. (2015), who found that the 'flavonoid biosynthesis' pathway plays an important role in the fading of red color in 'Red Bartlett' pear and in pigmentation of the *Litchi* pericarp. Another pathway with significantly enriched DEGs was 'porphyrin and chlorophyll metabolism' (Fig. 3), and upregulation of this pathway most likely contributes to the increased chlorophyll content detected in the greening of 'Xinlimei' radish taproot skin (Fig. 1). DEGs in 'carbon fixation in photosynthetic organisms', 'photosynthesis' and 'photosynthesis-antenna proteins' pathways were also significantly enriched, showing that the taproot skin can conduct photosynthesis with the increase in chlorophyll content that occurs in the greening process. Overall, the results of KEGG enrichment analysis of DEGs were consistent with the changes in anthocyanin and chlorophyll contents during skin color changes in 'Xinlimei' taproot. Therefore, we herein focus mainly on analyzing those genes responsible for anthocyanin and chlorophyll metabolism.

The anthocyanin biosynthetic pathway has been extensively studied in many plants, and most genes in radish have been isolated based on transcriptome datasets (Muleke et al., 2017; Sun et al., 2018). In the present work, we identified anthocyanin metabolism-related genes at the whole-genome level and compared their expression; thus, gene copies not expressed in the tissue used for RNA-Seq could be identified. Most genes were found to be present in more than one copy in the radish genome (Fig. 4B), which might be caused by tandem duplication or whole-genome triplication after the divergence of radish and *A. thaliana*. In this study, transcriptome analysis showed that the expression patterns of genes catalyzing the initial two steps of the anthocyanin biosynthetic pathway, *PAL* and *C4H*, did not correlate with the degradation of anthocyanins. Previous research on *Litchi* pericarp and radish taproot flesh coloration has also indicated differential expression patterns for *PAL* and *C4H* (Lai et al., 2015; Sun et al., 2018). FLS may be involved in the flavonol pathway, a branch of the anthocyanin biosynthesis pathway. Indeed, *FLS* was found to be significantly downregulated at SS1 and SS3 compared with SS2, which is different from a previous study reporting that reduced anthocyanin levels in 'Red Bartlett' pear are associated with decreased anthocyanin synthesis and increased *FLS* expression (Wang et al., 2017a,b). Thus, although the anthocyanin biosynthesis pathway appears to be conserved among different species, some diversity in gene expression still exists. Except for *PAL* and *C4H*, the expression levels of other anthocyanin biosynthetic genes (i.e., 4CL, *CHS*, *CHI*, *F3H*, *DFR*, *ANS*, and *UFGT*) correlated strongly with anthocyanin degradation.

Anthocyanins are synthesized in the cytosol and must be transported to the acidic vacuole for their rich colors to be displayed (Winkel-Shirley, 2001). *AtTT19* encodes a GST that functions as a carrier to transport anthocyanins from the cytosol to the tonoplast (Sun et al., 2012), and we identified a homologous gene in radish, *Rsa10018713*, with expression patterns that strongly correlated with the degradation of anthocyanins. In *A. thaliana*, the MATE transporter TT12 appears to be involved in proanthocyanidin transport (Marinova et al., 2007), and it has been previously reported that the homologous gene in radish, *RsMATE9*, might be involved in the transport of anthocyanins (Muleke et al., 2018). Nonetheless, the report by Sun et al. (2018) and our present research (Table S2) indicate that *RsMATE9* (*Rsa10029550*) is not expressed in the 'Xinlimei' taproot. Hence, RsTT19, but not RsMATE9, may be involved in anthocyanin transport, at least in the taproot skin of radish cultivar 'Xinlimei'. Our result is supported by Hu et al. (2016), who reported that the gene in *Litchi* homologous to *AtTT19*, GST4, complements the anthocyanin-less phenotype of the *A. thaliana tt19* mutant.

A previous study indicated that peroxidases are likely involved in anthocyanin degradation in plants (Zipor et al., 2015). Our present study identified a peroxidase-encoding gene *Rsa10017424*, that may be involved in anthocyanin degradation in radish because its expression levels in SS2 and SS3 were significantly higher than that in SS1. These results suggest that decreased anthocyanin biosynthesis and increased anthocyanin degradation likely contribute to the red skin color fading of 'Xinlimei' radish taproots.

Anthocyanin biosynthesis is regulated by a series of transcription factors, particularly the MYB-bHLH-WD40 complex (Koes et al., 2005). Through combined phylogenetic and expression analyses, we found that decreased expression levels of *RsMYB1* and *RsTT8*, but not *RsWD40*, which suppresses expression of anthocyanin biosynthesis structural genes, resulted in red color fading in the 'Xinlimei' taproot skin. Furthermore, a previous study reported that *RsTT8* interacts with *RsMYB1* and coregulates expression of *RsCHS* and *RsDFR* (Lim et al., 2017).

Increased chlorophyll content and enrichment of the 'porphyrin and chlorophyll metabolism' pathway were associated with the greening process of 'Xinlimei' radish taproot skin (Figs. 1 and 3). Therefore, to identify key genes responsible for greening, we identified and analyzed chlorophyll metabolism gene expression in radish. To our knowledge, the chlorophyll metabolism pathway in radish is first reported in the present study. During the greening process, chlorophyll biosynthesis genes, i.e., *HEMA1*, *HEMA2*, *HEMG1*, *HEMG2*, *CHLH*, *CHLD*, *CHLI1*, *CHLI2*, *CHLM*, *CRD1*, *PORB*, *PORC*, *CHLG*, and chlorophyll cycle genes, i.e., *HCAR*, *CAO*, *NYC1* and *NOL*, were significantly upregulated. However, chlorophyll degradation genes, including *CLH1*, *CLH2*, *RCCR* and *SGR*, were also significantly upregulated in the greening process. These results indicate that chlorophyll biosynthesis and degradation are maintained in a dynamic balance in green skin. A previous study indicated that this balance is important for the normal growth of leaves (Shimoda et al., 2016).

Expression of chlorophyll biosynthesis genes is positively or negatively regulated by transcription factors; 13 transcription factors were identified in the present study, and their expression was analyzed. Eleven (i.e. *ORE1*, *ACR5*, *ACR6*, *PIF1*, *CGA1*, *ANAC046*, *EIN3*, *FLU*, *PIF3*, *ARC3* and *GNC*) were excluded as key genes responsible for radish taproot skin greening because of low expression levels or because their expression patterns did not significantly change during the greening process. Nonetheless, *AtGLK1 AtGLK2* significantly higher expression

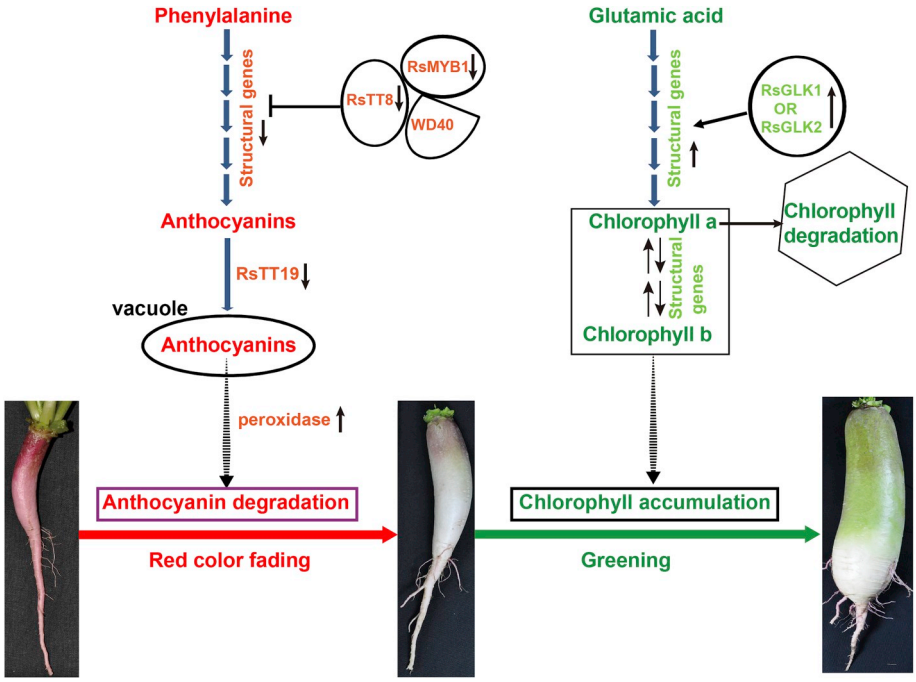

Fig. 8. The proposed model indicating the mechanisms of color changes in 'Xinlimei' radish taproot skin. *RsMYB1 RsTT8 RsTT19 RsGLK1 RsGLK2*. (For interpretation of the references to color in this figure legend, the reader is referred to the Web version of this article.)

levels *AtGLK1* and *AtGLK2* displayed at the green skin stage than at the red and white skin stages, respectively. A previous report indicated that *AtGLK1* and *AtGLK2* are functionally redundant in regulating chloroplast development, as single mutants do not exhibit phenotypic variation (Fitter et al., 2002). These results suggest that *RsGLK1* and *RsGLK2* are key genes positively regulating chlorophyll accumulation in the radish taproot during maturation. RT-qPCR results agreed with the profiles obtained by RNA-Seq, suggesting that the results obtained in the present study through analysis of high-throughput sequencing data were reliable (Fig. S2).

5. Conclusions

To reveal the molecular mechanisms underlying color changes in the skin of 'Xinlimei' radish taproot, transcriptome analyses were performed using RNA-Seq technology. Our results indicate that anthocyanin and chlorophyll metabolism pathways play important roles in color changes, and candidate genes involved in these processes were identified. A hypothetical model illustrating the molecular mechanisms of color changes is presented in Fig. 8. In the model, decreased levels of *RsMYB1* and *RsTT8* expression suppress formation of the MBW complex, resulting in further reduction in the expression levels of anthocyanin biosynthetic genes and decreased production of pigments. Downregulation of the anthocyanin transporter gene *RsTT19* results in reduced anthocyanin accumulation in vacuoles, whereas upregulation of predicted peroxidase-encoding genes promotes anthocyanin degradation. Increased expression of *RsGLK1* and *RsGLK2* activates the chlorophyll biosynthesis pathway, which results in chlorophyll accumulation exceeding its degradation, despite increased expression levels of genes involved in chlorophyll degradation. The decreased biosynthesis and increased degradation of anthocyanin, combined with higher levels of chlorophyll biosynthesis, cause red color fading and greening of the 'Xinlimei' taproot skin.

Conflicts of interest

The authors declare that the research was conducted in the absence of any commercial or financial relationships that could be construed as a potential conflict of interest.

Author contributions

Conceived and designed the experiments: XL, TL. Performed the experiments: TL, JS,YS. Analyzed the data: TL, XZ, XL, YZ,HW. Wrote the paper: TL, XL. All authors read and approved the final manuscript.

Data access

RNA-Seq data are available at EMBL/NCBI/SRA (accession number PRJNA505376).

Acknowledgements

This work was supported by grants from the National Key Research and Development Program of China (2016YFD0100204-02), National Natural Science Foundation of China (31801858), China Postdoctoral Science Foundation Funded Project (2017M620971) and the Science and Technology Innovation Program of the Chinese Academy of Agricultural Sciences (CAAS-XTCX2016016-4-4, CAAS-XTCX2016001-5-2, and,CAAS-XTCX2016017).

Appendix A. Supplementary data

Supplementary data to this article can be found online at https://doi.org/10.1016/j.plaphy.2019.04.006.

References

Abolhassani Rad, S., Clayton, E.J., Cornelius, E.J., Howes, T.R., Kohalmi, S.E., 2018. Moonlighting proteins: putting the spotlight on enzymes. Plant Signal. Behav. 13, e1517075.
Adhikari, N.D., Froehlich, J.E., Strand, D.D., Buck, S.M., Kramer, D.M., Larkin, R.M., 2011. GUN4-Porphyrin complexes bind the CNH/GUN5 subunit of Mg-chelatase and promote chlorophyll biosynthesis in *Arabidopsis*. Plant Cell 23, 1449–1467.
Beale, S.I., 2005. Green genes gleaned. Trends Plant Sci. 10 (7), 309–312.
Cao, K., Ding, T., Mao, D., Zhu, G., Fang, W., Chen, C., Wang, X., Wang, L., 2018.

Transcriptome analysis reveals novel genes involved in anthocyanin biosynthesis in the flesh of peach. Plant Physiol. Biochem. 123, 94–102.
Chen, F.B., Xing, C.Y., Huo, S.P., Cao, C.L., Yao, Q.L., Fang, P., 2016. Red pigment content and expression of genes related to anthocyanin biosynthesis in radishes (*Raphanus sativus* L.) with different colored flesh. J. Agric. Sci. 8 (8), 126–135.
Chu, H., Jeong, J.C., Kim, W.J., Chung, D.M., Jeon, H.K., Ahn, Y.O., Kim, S.H., Lee, H.S., Kwak, S.S., Kim, C.Y., 2013. Expression of the sweetpotato R2R3-type *IbMYB1a* gene induces anthocyanin accumulation in *Arabidopsis*. Physiol. Plantarum 148 (2), 189–199.
Deng, W., Wang, Y., Liu, Z., Cheng, H., Xue, Y., 2014. HemI: a toolkit for illustrating heatmaps. PLoS One 9 (11), e111988. https://doi.org/10.1371/journal.pone.0111988.
Fitter, D.W., Martin, D.J., Copley, M.J., Scotland, R.W., Langdale, J.A., 2002. GLK gene pairs regulate chloroplast development in diverse plant species. Plant J. 31, 713–727.
Gomez, C., Conejero, G., Torregrosa, L., Cheynier, V., Terrier, N., Ageorges, A., 2011. *In vivo* grapevine anthocyanin transport involves vesicle-mediated trafficking and the contribution of anthoMATE transporters and GST. Plant J. 67 (6), 960–970.
Gomez, C., Terrier, N., Torregrosa, L., Vialet, S., Fournier-Level, A., Verries, C., Souquet, J.M., Mazauric, J.P., Klein, M., Cheynier, V., Ageorges, A., 2009. Grapevine MATE-type proteins act as vacuolar H^+-dependent acylated anthocyanin transporters. Plant Physiol. 150 (1), 402–415.
Gonzalez, A., Zhao, M.Z., Leavitt, J.M., Lloyd, A.M., 2008. Regulation of the anthocyanin biosynthetic pathway by the TTG1/bHLH/Myb transcriptional complex in *Arabidopsis* seedlings. Plant J. 53 (5), 814–827.
Hichri, I., Barrieu, F., Bogs, J., Kappel, C., Delrot, S., Lauvergeat, V., 2011. Recent advances in the transcriptional regulation of the flavonoid biosynthetic pathway. J. Exp. Bot. 62, 2465–2483.
Hu, B., Zhao, J.T., Lai, B., Qin, Y.H., Wang, H.C., Hu, G.B., 2016. *LcGST4* is an anthocyanin-related glutathione *S-transferase* gene in *Litchi chinensis* Sonn. Plant Cell Rep. 35 (4), 831–843.
Jeong, Y., Kim, N., Ahn, B., Oh, M., Chung, W., Chung, H., Jeong, S., Lim, K., Hwang, Y., Kim, G., Baek, S., Choi, S., Hyung, D., Lee, S., Sohn, S., Kwon, S., Jin, M., Seol, Y., Chae, W., Choi, K., Park, B., Yu, H., Mun, J., 2016. Elucidating the triplicated ancestral genome structure of radish based on chromosome-level comparison with the Brassica genomes. Theor. Appl. Genet. 129, 1357–1372.
Klein, M., Burla, B., Martinoia, E., 2006. The multidrug resistance-associated protein (MRP/ABCC) subfamily of ATP-binding cassette transporters in plants. FEBS Lett. 580 (4), 1112–1122.
Koes, R., Verweij, W., Quattrocchio, F., 2005. Flavonoids: a colorful model for the regulation and evolution of biochemical pathways. Trends Plant Sci. 10 (5), 236–242.
Lai, B., Hu, B., Qin, Y.H., Zhao, J.T., Wang, H.C., Hu, G.B., 2015. Transcriptomic analysis of *Litchi chinensis* pericarp during maturation with a focus on chlorophyll degradation and flavonoid biosynthesis. BMC Genomics 16, 225. https://doi.org/10.1186/s12864-015-1433-4.
Li, R., Yu, C., Li, Y., Lam, T.W., Yiu, S.M., Kristiansen, K., Wang, J., 2009. SOAP2: an improved ultrafast tool for short read alignment. Bioinformatics 25 (15), 1966–1967.
Lim, S.H., Kim, D.H., Kim, J.K., Lee, J.Y., Ha, S.H., 2017. A radish basic helix-loop-helix transcription factor, RsTT8 acts a positive regulator for anthocyanin biosynthesis. Front. Plant Sci. 8, 1917. https://doi.org/10.3389/fpls.2017.01917.
Lim, S.H., Song, J.H., Kim, D.H., Kim, J.K., Lee, J.Y., Kim, Y.M., Ha, S.H., 2016. Activation of anthocyanin biosynthesis by expression of the radish R2R3-MYB transcription factor gene *RsMYB1*. Plant Cell Rep. 35 (3), 641–653.
Liu, T.J., Cheng, Z.H., Meng, H.W., Ahmad, I., Zhao, H.L., 2014. Growth, yield and quality of spring tomato and physicochemical properties of medium in a tomato/garlic intercropping system under plastic tunnel organic medium cultivation. Sci. Hortic. 170 (3), 159–168.
Liu, T.J., Zhang, X.H., Yang, H.H., Agerbirk, N., Qiu, Y., Wang, H.P., Shen, D., Song, J.P., Li, X.X., 2016. Aromatic glucosinolate biosynthesis pathway in *Barbarea vulgaris* and its response to *Plutella xylostella* infestation. Front. Plant Sci. 7, 83. https://doi.org/10.3389/fpls.2016.00083.
Livak, K.J., Schmittgen, T.D., 2001. Analysis of relative gene expression data using real-time quantitative PCR and the $2^{-\Delta\Delta CT}$ method. Methods 25, 402–408. https://doi.org/10.1006/meth.2001.1262.
Majee, M., Kumar, S., Kathare, P.K., Wu, S., Gingerich, D., Nayak, N.R., Salaita, L., Dinkins, R., Martin, K., Goodin, M., 2018. KELCH F-BOX protein positively influences Arabidopsis seed germination by targeting PHYTOCHROME-INTERACTING FACTOR1. Proc. Natl. Acad. Sci. U.S.A. 115, 201711919.
Marinova, K., Pourcel, L., Weder, B., Schwarz, M., Barron, D., Routaboul, J.M., Debeaujon, I., Klein, M., 2007. The *Arabidopsis* MATE transporter TT12 acts as a vacuolar flavonoid/H^+-antiporter active in proanthocyanidin-accumulating cells of the seed coat. Plant Cell 19 (6), 2023–2038.
Mortazavi, A., Williams, B.A., Mccue, K., Schaeffer, L., Wold, B., 2008. Mapping and quantifying mammalian transcriptomes by RNA-Seq. Nat. Methods 5, 621–628.
Muleke, E.M.M., Cheng, W., Xu, L., Wang, Y., Karanja, B.K., Zhu, X., Cao, Y., Liu, L., 2018. Identification and transcript analysis of MATE genes involved in anthocyanin transport in radish (*Raphanus sativus* L.). Sci. Hortic. 238, 195–203.
Muleke, E.M.M., Fan, L., Wang, Y., Xu, L., Zhu, X., Zhang, W., Cao, Y., Karanja, B.K., Liu, L., 2017. Coordinated regulation of anthocyanin biosynthesis genes confers varied phenotypic and spatial-temporal anthocyanin accumulation in radish (*Raphanus sativus* L.). Front. Plant Sci. 8, 1243. https://doi.org/10.3389/fpls.2017.01243.
Naoumkina, M.A., Zhao, Q., Gallego-Giraldo, L., Dai, X.B., Zhao, P.X., Dixon, R.A., 2010. Genome-wide analysis of phenylpropanoid defence pathways. Mol. Plant Pathol. 11 (6), 829–846.
Oren-Shamir, M., 2009. Does anthocyanin degradation play a significant role in determining pigment concentration in plants? Plant Sci. 177 (4), 310–316.
Park, N.I., Xu, H., Li, X., Jang, I.H., Park, S., Ahn, G.H., Lim, Y.P., Kim, S.J., Park, S.U., 2011. Anthocyanin accumulation and expression of anthocyanin biosynthetic genes in radish (*Raphanus sativus*). J. Agric. Food Chem. 59 (11), 6034–6039.
Patel, R.K., Jain, M., 2012. NGS QC Toolkit: a toolkit for quality control of next generation sequencing data. PLoS One 7 (2), e30619. https://doi.org/10.1371/journal.pone.0030619.
Shimoda, Y., Ito, H., Tanaka, A., 2016. Arabidopsis STAY-GREEN, Mendel's green cotyledon gene, encodes magnesium-dechelatase. Plant Cell 28, 2147–2160.
Sun, Y., Li, H., Huang, J., 2012. *Arabidopsis* TT19 functions as a carrier to transport anthocyanin from the cytosol to tonoplasts. Mol. Plant 5 (2), 387–400.
Sun, Y.Y., Wang, J.L., Qiu, Y., Liu, T.J., Song, J.P., Li, X.X., 2018. Identification of 'Xinlimei' radish candidate genes associated with anthocyanin biosynthesis based on a transcriptome analysis. Gene 657, 81–91.
Tamura, K., Peterson, D., Peterson, N., Stecher, G., Nei, M., Kumar, S., 2011. MEGA5: molecular evolutionary genetics analysis using maximum likelihood, evolutionary distance, and maximum parsimony methods. Mol. Biol. Evol. 28, 2731–2739.
Wang, L.K., Feng, Z.X., Wang, X., Wang, X.W., Zhang, X.G., 2009. DEGseq: an R package for identifying differentially expressed genes from RNA-seq data. Bioinformatics 26 (1), 136–138.
Wang, Z., Cui, Y., Vainstein, A., Chen, S., Ma, H., 2017a. Regulation of fig (*Ficus carica* L.) fruit color: metabolomic and transcriptomic analyses of the flavonoid biosynthetic pathway. Front. Plant Sci. 8, 1990. https://doi.org/10.3389/fpls.2017.01990.
Wang, Z., Du, H., Zhai, R., Song, L., Ma, F., Xu, L., 2017b. Transcriptome analysis reveals candidate genes related to color fading of 'Red Bartlett' (*Pyrus communis* L.). Front. Plant Sci. 8, 455. https://doi.org/10.3389/fpls.2017.00455.
Winkel-Shirley, B., 2001. Flavonoid biosynthesis. A colorful model for genetics, biochemistry, cell biology, and biotechnology. Plant Physiol. 126 (2), 485–493.
Yasumura, Y., Langdale, J.A., 2005. A conserved transcription factor mediates nuclear control of organelle biogenesis in anciently diverged land plants. Plant Cell 17, 1894–1907.
Yi, G., Kim, J.S., Park, J.E., Shin, H., Yu, S.H., Park, S., Huh, J.H., 2018. MYB1 transcription factor is a candidate responsible for red root skin in radish (*Raphanus sativus* L.). PLoS One 13, e0204241.
Zhang, X.H., Yue, Z., Mei, S.Y., Qiu, Y., Yang, X.H., Chen, X.H., Cheng, F., Wu, Z.Y., Sun, Y.Y., Yi, J., Liu, B., Shen, D., Wang, H.P., Cui, N., Duan, Y.D., Wu, J., Wang, J.L., Gan, C.X., Wang, J., Wang, X.W., Li, X.X., 2015. A *de novo* genome of a Chinese radish cultivar. Hortic. Plants J. 1 (3), 155–164.
Zipor, G., Duarte, P., Carqueijeiro, I., Shahar, L., Ovadia, R., Teper-Bamnolker, P., Eshel, D., Levin, Y., Doron-Faigenboim, A., Sottomayor, M., Oren-Shamir, M., 2015. *In planta* anthocyanin degradation by a vacuolar class III peroxidase in *Brunfelsia calycina* flowers. New Phytol. 205 (2), 653–665.